Canopy airspace of riparian forest mitigates soil N2O emission during hot moments

Ülo Mander (ulo.mander@ut.ee)
University of Tartu https://orcid.org/0000-0003-2340-6989

Alisa Krasnova
University of Tartu

Jordi Escuer-Gatius
Estonian University of Life Sciences

Mikk Espenberg
University of Tartu https://orcid.org/0000-0003-0469-6394

Thomas Schindler
University of Tartu

Katerina Machacova
Global Change Research Institute CAS https://orcid.org/0000-0002-8289-169X

Jaan Pärn
University of Tartu https://orcid.org/0000-0001-6507-8894

Martin Maddison
University of Tartu

Patrick Megonigal
Smithsonian Institution https://orcid.org/0000-0002-2018-7883

Mari Pihlatie
University of Helsinki https://orcid.org/0000-0001-6035-3949

Kuno Kasak
University of Tartu

Ülo Niinemets
Estonian University of Life Sciences

Heikki Junninen
Institute of Physics, University of Tartu https://orcid.org/0000-0001-7178-9430

Kaido Soosaar
University of Tartu

Article

Keywords: automated chambers, eddy covariance, grey alder, QCLAS, soil flux, stem flux

Posted Date: October 7th, 2020

DOI: https://doi.org/10.21203/rs.3.rs-85457/v1

Abstract

Riparian forests are known as hot spots of N cycling in landscapes and climate warming speeds up the cycle. Here we present results from the first multi-annual high temporal-frequency study of soil, stem and ecosystem (eddy covariance) fluxes of N_2O from a typical riparian forest in Europe.

Hot moments (extreme events of N_2O emission) last a quarter of the study period but contribute more than a half of soil fluxes. For the first time we demonstrate that high soil emissions of N_2O do not reach the ecosystem level. During the drought onset, soil N_2O emission peaks at intermediate soil water content. Rapid water content change is the main determinant of the emissions. The freeze–thaw period is another hot moment. However, according to the eddy covariance measurements the riparian forest is a modest source of N_2O. We propose photochemical reactions and dissolution in canopy-space water as consumption mechanisms.

Introduction

Forests are important regulators of carbon dioxide (CO_2) fluxes[1] but their role in regulating other greenhouse gas (GHG) budgets, in particular for nitrous oxide (N_2O), is still largely unknown[2]. The accelerated increase in atmospheric N_2O concentrations (from a pre-industrial concentration of 270 ppbv to 328 ppbv in 2016[3] is of concern not only because N_2O is responsible for approximately 6% of global radiative forcing from anthropogenic GHGs. Its ozone-depletion potential outweighs the sum of emissions from all other ozone-depleting substances controlled by the Montreal Protocol[4]. Thus, N_2O is the most dangerous stratospheric ozone-layer depleting agent in the 21st century[5], and the third most important GHG having a global warming potential 296 times (100-yr lifetime adjustment, with feedbacks) that of CO_2[3].

Riparian forests provide important ecosystem services[6]. They regulate runoff flow, prevent nonpoint source pollutants from entering water bodies, enhance the in-stream processing of both nonpoint and point source pollutants, create habitats for many species, support landscape connectivity, and serve as recreational and cultural-educational areas[7]. Their multifunctional role reinforces current policy in several countries endorsing riparian forest buffers as best management practice subsidizing riparian reforestation for stream restoration and water quality[8]. One of the main functions of riparian forests in agricultural landscapes is removal of excess nitrate (NO_3^-) via complete denitrification[9], converting NO_3^- to N_2 gas. However, incomplete denitrification can result in the production of N_2O, a powerful greenhouse gas. Generally, a variety of nitrogen cycle processes can produce N_2O[10] but in riparian zones, denitrification has been found the most important source of N_2O[11,9].

Grey alder (*Alnus incana* (L.) Moench) is a fast-growing tree species typically found in riparian zones, with great potential for short-rotation bioenergy forestry[12]. Their symbiotic dinitrogen (N_2) fixation ability

makes alders important for the regulation of the nitrogen (N) cycle[13,12]. Grey alder forests are widely distributed in Europe and North America[14] (Supplementary Fig. S1) whereas in Europe they are often dominating communities in riparian zones[15]. In Europe there are 15,000 km^2 of *Alnus incana* subsp. *incana* forests[14].

N_2O fluxes measured in forest soils[16-20] varied from 0.00054 mg N_2O-N m^{-2} h^{-1} in a birch plantation in China[20] to 0.082 mg N_2O-N m^{-2} h^{-1} in a spruce forest under high N deposition in Germany[18]. In general, temperate forest soils emit 1.57 kg N_2O ha^{-1} yr^{-1} whereas in boreal forests the net emission is four times lower and in tropical forests three times higher than that in temperate forests[21].

Remarkably high net average N_2O fluxes from soil have been measured in riparian forests[22], and most of the studies were conducted in riparian alder stands[23-28].

For most of soil N_2O flux studies, manual chambers have been used, and few investigations are based on automated chambers[19,28] whereas Pihlatie et al[16,29] compared fluxes measured by chambers and the eddy covariance (EC) technique.

Hot spots and hot moments (extreme events of emissions) largely determine spatio-temporal variation of N_2O emissions from soils[30], and soil water content (SWC) is a leading factor controlling all the hot moments. A SWC value of 50–80% has been shown to be optimal for soil N_2O emissions in forests on both mineral soils[31] and organic soils[32]. Therefore, depending on the initial moisture, both flooding and drought can induce hot moments in tropical forests[33,34]. Drought has been observed to decrease soil N_2O emissions and account for soil N_2O consumption[35,36]. The majority of these studies have been conducted in relatively dry mineral soils and only few focused on wetter conditions of organic soils[17,33] or Gleysols[28]. Air and topsoil temperatures also play important role in determining hot moments of soil N_2O fluxes but mostly in colder climates37. Only few studies have considered the impact of hot moments on N_2O emissions from tree stems[38,28].

Freeze–Thaw cycles are well-known to substantially increase N_2O emission from soils whereas in agricultural soils their impact is more remarkable than in forests[39,40]. In forests, the Freeze–Thaw periods can significantly contribute to the annual N_2O budgets[39,41,42]. Thinner snow cover in forests always causes N_2O soil emissions to increase. In northern deciduous forests it can be due to the increase in Freeze–Thaw cycles[43]. Although there are several hypotheses explaining the impact of Freeze–Thaw cycles on soil N_2O emissions[40,44,45], a generally acceptable theory of Freeze–Thaw impact on N_2O fluxes is still missing.

Several investigations are available on N_2O emissions from tree stems in laboratory[46,47], using in situ manual stem chambers[48-52,38,28] and automated chambers[53]. The studies demonstrate that N_2O can be

emitted or consumed by stems whereas flooding significantly but only temporarily increases emissions[46,47,38,28], especially from the lower parts of stems[38,28]. Some studies have found evidence that N_2O emitted from tree stems may originate from the soil[49]. However, no study has quantified the contribution of N_2O fluxes from stems in the N_2O budget of a forest ecosystem and moreover, factors controlling N_2O fluxes from stems remain unclear[52]. It seems that N_2O exchange from boreal tree stems might follow the tree physiological activity, especially the processes connected to CO_2 exchange[51]. For instance, it is unclear whether N_2O exchange between stems and atmosphere is ruled by microbial or fungal activity within the tree stem or by plant biophysical process[54].

Only few studies could be found on EC measurements of N_2O fluxes[55,56]. Long-term N_2O flux measurements above tree canopies using eddy covariance technology are still missing. No previous complex investigations on forest ecosystems' N_2O budgets (soil and tree stem flux studies with EC measurements above the canopy) could be found. Nevertheless, estimation of the N_2O balance in different forest ecosystems under various environmental conditions is essential to understand their impact on climate.

This paper is aimed to analyze long-term relationship of continuously measured N_2O fluxes with key environmental factors in a riparian deciduous forest of hemiboreal zone. The second objective is to analyze the role of hot moments in temporal pattern of N_2O fluxes. We hypothesize that: (1) the studied riparian forest is a net N_2O source; (2) soil water content- and temperature-related hot moments play important role in long-term pattern of N_2O fluxes, (3) EC-measured N_2O fluxes are coherent to the sum of soil and stem fluxes, (4) N_2O fluxes from stems are positively correlated with soil N_2O fluxes, and (5) there is an optimal range of soil moisture for N_2O fluxes from soils.

Results

2.1 Environmental characteristics of hot moments

Based on high emissions of N_2O, dynamics of soil volumetric water content (further referred to as soil water content, SWC) and near-ground air temperature we identified four hot moments and related them to soil and environmental variables (see numbers in Fig. 1): Wet (1) , Dry (2) with Drought Onset (2a), Freeze–thaw (3), and Dry-minor (4). The main criterion for the hot moments was rapid increase in N_2O emissions of any source. The hot moments were characterised according to environmental factors. For instance, for Wet, Dry and Dry-minor periods, change in SWC was the main characteristic while for Freeze–Thaw, near-floor air temperature was used as the second factor for distinguishing this hot moment (Fig. 1). Since during the Freeze–Thaw the soil temperature at 0-10cm was almost constant, near-ground air temperature was more significant determinant.

Anomalies from the mean of each hot moment period illustrate the pattern of fluxes during the hot moments (Fig. 2). At the end of the Freeze–Thaw period, the rising SWC driven by snow melt became a

leading determinant (Fig. 2). Except the Wet period, during all hot moments only soil N_2O flux showed significant peaks. During the Wet period remarkable increase was observed also in the stem fluxes and EC-based ecosystem fluxes.

2.2 Soil N_2O fluxes

N_2O fluxes varied from -0.040 to 1.50 mg N_2O-N m^{-2} h^{-1}. The heatmap in Figure 3 presents spatial and temporal variation of these values, showing that across the whole study period, no remarkable differences between the values measured in individual chambers were observed. However, chambers 3, 8, 9 and 10 located in lower positions (10-20 cm from the average soil surface) showed somewhat higher values, especially in spring and autumn (Fig. 3). Temporal variation in soil N_2O fluxes align with the four hot moments we identified which showed remarkably higher flux values. Except for the Freeze–Thaw period in February-March 2019 negative N_2O fluxes occurred primarily in the winter months, accounting for 43% of monthly values in February 2018 and January 2019 (Fig. S2). The highest flux values (>0.10 mg N_2O-N m^{-2} h^{-1}) were observed in late spring, summer and autumn, accounting for a maximum of 38% of the measurements at the Drought Onset in May 2018 (Fig. S2). During this short period, in all individual chambers the daily average flux was >0.02 mg N_2O-N m^{-2} h^{-1} (Fig. 3).

During the whole study period the cumulative N_2O soil flux was 458.8 ± 7.7 mg N_2O-N m^{-2} (mean ± standard deviation) whereas hot moments contributed 55.9% of the whole flux (Table 1). During the calendar years 2018 and 2019, 196.3 ± 7.1 and 221.0 ± 12.4 mg N_2O-N m^{-2} y^{-1} was emitted (Supplementary Table S1). When considering the two full years of the study (Sept. 2017 – Sept. 2018 and Sept. 2018 – Sept. 2019), the corresponding cumulative flux values were 215.5 ± 7.7 and 221.4 ± 12.2 mg N_2O-N m^{-2} y^{-1} (Fig. 4; Table S1)

Except for the Dry hot moments, no remarkable diurnal pattern of soil N_2O fluxes were found. During the both hot moments average day-time values were up to 100 higher than those in the night-time showing also higher variability than in other months (Fig. S3).

2.3. Stem N_2O fluxes

Stem fluxes of N_2O measured during 52 campaigns averaged over all measured heights and expressed per m^2 of forest ground varied between −0.00028 and 0.0228 mg N_2O-N m^{-2} h^{-1}. The highest emissions were measured on the lowest position of tree stems whereas at higher positions (170 cm from ground) slight consumption was observed. The average ± standard error values of N_2O stem flux during the measurement period from September 2017 to December 2018 were 0.00022 ± 0.00007 mg N_2O-N m^{-2} h^{-1}. Although the absolute values of stem fluxes were low, both spatial and temporal variability of stem fluxes were remarkable. Spatial variation arose from 3 tree stems among the 12 measured ones were consuming N_2O (−0.00002 ± 0.00001 mg N_2O-N m^{-2} h^{-1}) whereas the rest showed always showed low emissions (0.00031 ± 0.00013 mg N_2O-N m^{-2} h^{-1}). No correlation between the stem fluxes and the spatial

variation of measured environmental data were found. The hot moments Wet and Dry contributed respectively 40.7% and 11,7% of total cumulative emissions during the whole stem measurement period (3.53 mg N_2O-N m^{-2}; Table 1). During the period from September 2017 to September 2018, a slight increase in cumulative values of stem fluxes appeared and at the end of the measurement period when only consumption of N_2O by stems was measured (Fig. 4).

2.4. Ecosystem level N_2O fluxes (Eddy covariance)

The daily sums of ecosystem N_2O fluxes varied in relatively small range, from −0.60 to 1.16 mg N_2O-N m^{-2} d^{-1}. Gap-filled data covered 24% of the whole measurement period (Fig. 5). While the peaks of soil N_2O fluxes were not reflected at the ecosystem scale (Figs. 1, 2 and 4), ecosystem N_2O fluxes showed a seasonal pattern with the highest positive fluxes in spring (March–April) and autumn months (October–November) and small close to zero values over the both summers (Figs. 5 and S4). Likewise, higher values were observed during the 'Wet' hot moment with 19.8% of total cumulative EC flux of the whole study period (87.3 mg N_2O-N m^{-2}; Figs. 4 and 5, Table 1). We observed a distinctive diurnal pattern with small negative fluxes during the morning hours (8–12) in summer months of both years. We observed no diurnal pattern neither in simultaneous soil fluxes nor in EC fluxes of autumn, winter or spring months. The hourly average flux values ranged from −0.029 to 0.029 mg N_2O-N m^{-2} h^{-1} (Fig. S3).

2.5. Relationships of N_2O flux and environmental parameters

The main factors related to N_2O soil fluxes in this ecosystem were SWC and soil temperature (Fig. 6a). Based on the full data set measured during the study period, there was an optimal SWC value of about 0.5 m^3 m^{-3} (50%) at which the soil flux was the highest (Fig. 6b). The relationship between the soil surface temperature and soil N_2O flux was more complex showing two peaks: one at 0-4^oC and a second one at 13-14^oC (Fig. 6c). The first peak corresponds to the Freeze–Thaw period and the second one represents the Dry and Dry-minor hot moments.

During the Dry hot moment, the correlation between the SWC and soil N_2O emission was very strong showing a clear peak at SWC values between 0.35 and 0.5 % (Fig. 7).

N_2O stem fluxes were influenced by SWC, however, a positive relationship was found only during the Wet period and it was not statistically significant. We did not find any significant relationships between ecosystem N_2O fluxes and environmental parameters (air and soil temperature, SWC, wind speed) or gross primary production (GPP) on half-hourly scale. However, a general pattern of weekly average fluxes followed that of SWC with the modifying influence of changes in air temperature (Fig. S4).

Discussion

N_2O emissions from terrestrial ecosystems are always irregular and highly variable at both temporal and spatial scale[10,19,57]. Therefore, consideration of hot moments and hot spots is essential to obtain an adequate long-term account of N_2O fluxes[30] and for inferring the mechanisms that drive these events under field conditions.

Soil water content was the main factor associated with hot moments of N_2O emission from soils, and it has been argued that drought and rewetting trigger such events by different mechanisms[58]. Likewise, we propose that hot moments in current study were caused by a variety of different mechanisms. Specifically, we identified the Wet period associated with increasing SWC, Drought periods associated with decreasing SWC and the Freeze–Thaw period based on fluctuating ground temperature around 0^oC and slight increases in SWC (Figs. 1 and 2). In all cases, SWC remained above 50%. We found that warmer conditions (Drought in our case) had a greater influence on emissions than wetter conditions (Wet), however, the combined effect of wetter and warmer conditions would be more offsetting than synergetic (Fig. 6) Analogous results were observed by Shrestha & Wang[37]. Likewise, a climate manipulation experiment in a post-harvest forest showed that wetting increased soil N_2O flux but not when combined with heating[59].

In our study, hot moments Dry and Freeze–Thaw contributed correspondingly 9 and 8–10 times higher soil N_2O emission than the period average (Fig. 2). In tropics, where the temperature is constantly high, soil N_2O fluxes increased markedly after the start of the wet season, while tree stem bases emitted N_2O throughout both dry and wet periods[38]. Likewise, automated measurements during a lab experiment with intact soil mesocosms from a temperate forest by Petrakis et al[60] observed an increase of up to four orders of magnitude in emissions following flooding pulses. In field conditions the effect of pulsing groundwater table on N_2O emissions from the soil was significantly lower[26].

Our results demonstrate that the highest soil N_2O fluxes were observed at the SWC value around 50% (Fig. 6b) which was most remarkable during the “Drought Onset” (Fig. 7). Although several studies have shown similar relationship[31,32], many studies have found contrasting trends working either in dry mineral soils (SWC <45%) or in the wet conditions (SWC >45%). Studies of the first group[35,36] have found drought-driven decrease of soil N_2O emissions. The drought in these conditions can make the forest soil into a sink of atmospheric N_2O[36] and if the dry period lasts several weeks, even rewetting will not increase the N_2O emission[35]. Studies focused on wetter conditions in organic soils with SWC >60% could observe a reverse relationship in which drying of the wet soils caused a significant increase in N_2O emissions[17,32]. During our 2.5-yr study period of continuous automated measurements in riparian gleyic soil we observed both trends: a substantial drought-driven increase of N_2O emissions in wet conditions (SWC >70%; Drought Onset episode) and a drought-driven decrease of N_2O emissions in dry conditions (SWC <45%; end of Dry period) with short–term emission peaks caused by precipitation (rewetting; Dry-minor; Fig. 2). In all cases, the highest emissions occurred when the SWC level passed the optimum value around 50%.

Lesser fluctuations of N_2O were observed in the beginning of the Wet period and during the hot moment Dry-minor, when the SWC fluctuated between 45 and 50% (Fig. 2).

During the Freeze–Thaw period a different complex of factors caused a substantial increase in N_2O emissions from soil. Several hypotheses have been posed to explain this phenomenon, the most common of which are: i) freeze–thaw disrupts soil aggregates exposing physically protected organic matter to be rapidly mineralized by microorganisms[40]; ii) large proportions of microorganisms, fine roots, and mycorrhiza die during the freeze[44], providing rapidly decomposable organic matter during the thaw; iii) the death of fine roots decreases the roots' competitive absorption of nitrate, the main source of N_2O[45].. However, the underlying mechanism involved in the pulse emissions of N_2O remains uncertain and further exploration is required[61].

Recent investigation reveals that the freeze–thaw related soil N_2O flux is high and could constitute a major component in annual budgets of different ecosystems[41]. In two hemiboreal forests growing on drained peat, one dominated by Norway spruce, and the other by downy birch, the wintertime freeze–thaw related N_2O release made up for 87% of the total annual emission[42]. Wagner-Riddle et al[62] estimated that neglecting freeze–thaw emissions can overlook 17 to 28% of global agricultural N_2O emissions. For forests, this has not been calculated. Likewise, in most models for calculating regional and/or global N_2O emissions, the wintertime freeze–thaw emissions are not accounted[63]..

The greatest increase in soil N_2O emission from Freeze–Thaw cycles was always observed during and shortly after the thawing[39,64,65]; however, the peaks lasted only for a short period (few days[65]). This was also the case in our investigations (Fig. 2). In addition, we could see that the SWC plays an important role in N_2O fluxes, especially at the end of the Freeze–Thaw period (Fig. 2). The snow-melt water increased the SWC close to 50% and initiated small pulsations of N_2O. A similar phenomenon at the same SWC values was described by Teepe et al[39]. Likewise, Teepe et al[41] demonstrated that during thawing, emissions of N_2O increased with the decrease in water-filled pore space (WFPS) of soil from 76% to 55% WFPS.

We observed the freeze–thaw effect only in February and March 2019 when the snow cover was sporadic and thin, and several open patches were frozen in the nighttime causing slight fluctuations in diurnal pattern of N_2O soil fluxes (Fig. S3). In contrast, in February and March 2018, there was a continuous snow cover of 20-30 cm under which the SWC was decreasing from 70% to 45% (Fig. S4), however, no significant emission of N_2O fluxes from the soil was observed (Fig. 2). Most likely, continuous thick snow cover buffered the topsoil temperature and stabilized the fluxes. Likewise, Groffman et al[43] demonstrated that sporadic and dynamic snow-cover during spring enhances N_2O pulses from soil and that the climate warming-induced decreasing snow cover might increase soil-atmosphere N_2O fluxes from northern forests.

The different hot moments were driven by different relationships with the environmental factors. During the Drought Onset, there was a strong negative correlation between speed of SWC decrease and N_2O flux (Fig. 8a). This relationship is a novel finding. Accordingly, the speed of the SWC decrease could be included in N_2O flux models for the drought period. This interpretation is supported by Barrat et al[58] review on drought and rewetting effects on soil N_2O fluxes indicating that the larger the WFPS change, the larger the N_2O pulse with the the largest emissions occurred at 70% WFPS. In our Freeze–Thaw period, a positive correlation between the near-floor air temperature and N_2O flux was observed (Fig. 8b) suggesting that temperature may play a dominant role in the initiation of the N_2O flux hot moments. Besides temperature, SWC and related oxygen (O_2) supply are important factors as shown in a model by Öquist et al[64] where anomalies of O_2 availability rather than temperature play the leading role in cold-period N_2O flux regulation.

Both droughts and freeze–thaw cycles change SWC and disturb the O_2 balance in soils initiating nitrifying microorganisms and retarding the full denitrification pathway ending with N_2[66]. The result is always the same – pulses of N_2O emission.

We did not observe meaningful diurnal patterns in soil N_2O fluxes during most of the study period, except for the Dry and Freeze–Thaw hot moments (Fig. S3). Likewise, in their meta-analysis of global terrestrial N_2O fluxes, Li et al[67] found no difference between day- and night-time fluxes.

The fluxes of N_2O from stems were relatively low compared to the soil fluxes and showed higher values during the Wet and Dry periods (Figs. 2 and 4). A few measurements from stems at 5 m height of six trees in the Dry period showed almost zero flux. The low stem flux was somewhat unexpected because in some previous studies alders have shown higher tree stem emissions compared to other temperate tree species[46,47,50,28]. However, in all previous studies flooding was the main factor initiating high N_2O fluxes from stems. For instance, Rusch & Rennenberg[46] found that immediately after flooding of the soil, N_2O flux from *Alnus glutinosa* seedlings showed a peak of 350 µmol N_2O m^{-2} h^{-1} (15.4 mg m^{-2} h^{-1}) but after more than 40 days of flooding it had decreased below the limit of detection. According to Machacova et al[47] flooding caused a dramatic transient increase of N_2O emission from stems of young *A. glutinosa* by a factor of 740.

Unexpectedly, the ecosystem flux measured by the EC technique above the forest canopy was relatively low and did not follow the variability in soil N_2O fluxes (Figs. 1, 2 & 5). During the Wet period one significant N_2O peak occurred, while emissions remained low during the rest of the period. Other hot moments did not lead to any increase in N_2O EC flux (Figs. 2, 5 and S4). However, there was a relationship between the EC flux and SWC (Fig. S4). During February and March 2018, the decreasing EC N_2O flux almost perfectly followed the decrease in SWC, and over the longer period from October 2018 until October 2020 the trends were similar (Fig. S4). Due to a lack of comparable studies on EC N_2O measurements in forest ecosystems, conventional comparison is impossible. However, comparison of

fluxes from all compartments measured may provide valuable information. The cumulative emission from ecosystem (87.3 mg N_2O-N m^{-2}) was 5.3 times smaller than the emission from the soil (458.8 mg N_2O-N m^{-2}; Table 1), whereas the difference between these two sources was constantly increasing throughout the whole study period (Fig. 4). During the 1.5-year period the cumulative flux from alder stems was 3.53 mg N_2O-N m^{-2}, which constituted only 0.77% of cumulative soil fluxes (Table 1). This is about the same level with the findings by Wen et al 2017[50] on *A. glutinosa* trees (1.1%).

Since the measurement frequency was sufficient to capture all the fluxes it is difficult to explain such a great difference between the soil and ecosystem level. During the Drought Onset episode in 2019, N_2O concentrations increased at wind-still nights (Fig. S5) and fluxes declined in the subsequent clear sunny days (Fig. S3b). The consumption could be explained by photochemical reactions, which have been observed in both boreal[68] and tropical forests[69]. The monthly sum of sunshine hours during our Drought Onset and Dry-minor hot moments was high (Fig. S6). Thus, during the hot moments photochemical reactions may have decreased the ecosystem (EC) flux of N_2O. In autumn, winter and spring the consumption of N_2O could be related to the high solubility of N_2O gas in water (1.0 ml gas per ml water at 5°C) which is a reason why significant quantities are transported from the soil in drainage water[70]. Likewise, Warneke et al[71] reported that absorption of N_2O by woodland soil water contributed up to a half of the total N_2O consumption in soil. Theoretically, it is possible that fog, which often appears in this ecosystem, can absorb part of the N_2O that was not measured by the EC system. Eugster et al[55] in its early EC study in a mixed forest also mentions that wetting of the canopy at fog can have strong influence on N_2O fluxes, but no clear evidence of absorption in fog has been reported yet. Likewise, Min et al[72] found that NOx fluxes from the forest canopy were smaller than measured soil NOx emissions and referred to the phenomenon as a “canopy reduction factor” which they applied to soil NOx emissions in large-scale models. The interpretation of these differences was a chemical conversion of NOx to other nitrogen oxides within the forest canopy. Fulgham et al[73] report that wet surfaces of leaves/needles and branches in a mixed forest control the vertical exchange of gases (volatile organic acids). Since the exchange velocity of these gases was well correlated with dew point depression (DPD) we compared the monthly average soil and EC fluxes of N_2O with DPD in our forest. We found that during the autumn and winter (except the Freeze–Thaw period) differences between soil and EC fluxes were lowest (Fig. S6).

We also checked whether the trees’ photosynthetic activity could be related to N_2O EC fluxes but the correlation analysis with gross primary production (GPP; obtained from the EC tower by LiCor system) did not show significant correlation neither throughout the whole study period nor at a monthly basis.

Almost all of previous upscaled annual rates of N_2O exchange between the atmosphere and forest ecosystem were based on soil emission values. Therefore, for the upscaling to annual and hectare level we used both a soil- and canopy-based approach. Based on the soil values, this riparian alder forest emitted on average 2.18 kg N_2O-N ha^{-1} y^{-1}. According to canopy-based calculations, the emission is only

0.26 kg N_2O-N ha^{-1} y^{-1}. Thus, both calculations show that this type of riparian forest is emitting several times less N_2O than the agricultural areas[4] or drained N-rich peatlands[32].

Upscaling these values to the whole *Alnus incana* subsp *incana* distribution area (15,000 km^2)[14], we estimate the total annual emissions of 3,270 (soil-based) or 390 tons (canopy-based) of N_2O-N a year. Thus, in addition to several ecosystem services which riparian alder forests can provide, they are low emitters of N_2O which make them attractive for riparian zone management

Conclusions

The outcomes of our long-term study support our hypothesis that this alder forest is a net source of N_2O. The second hypothesis on the role of hot moments in long-term pattern of N_2O fluxes was also supported – hot moments contributed about 56% of soil emissions throughout the whole study period. The third hypothesis was not supported – ecosystem (eddy covariance) flux was not coherent with the soil + stem fluxes. The stem flux was almost close to zero showing only some increase during the Wet period. In comparison to high soil N_2O emission, the ecosystem level emission was about 5.3 times lower. Photochemical reactions and dissolution in atmospheric water may be the consumption mechanisms behind that.

As hypothesized, soil N_2O flux peaked at 50% of SWC whereas during the Drought Onset the correlation was strong and N_2O flux mainly depended on speed of SWC change. During Freeze–Thaw, near-surface air temperature was the main factor of N_2O soil flux.

In the next decades we anticipate a global increase in frequency of disturbances causing hot moments of greenhouse gas emissions in terrestrial ecosystems. Our study reveals the importance of high-frequency field measurements across the year. Full understanding of nitrogen budgets of riparian forests cannot rely on soil level measurements only but must be combined with tree-stem, canopy and ecosystem-level EC fluxes. Identification of microorganisms and biogeochemical pathways associated with N_2O production and consumption is another future challenge.

Methods

5.1 Study site and set-up

The studied hemiboreal riparian forest is a 40-year old *Filipendula* type grey alder (*Alnus incana* (L.) Moench) forest stand grown on a former agricultural agricultural land. It is situated in the Agali Village (58°17’ N; 27°17’ E) in eastern Estonia within the Lake Peipsi Lowland[74].

The area is characterized by a flat relief with an average elevation of 32m a.s.l., formed from the bottom of former periglacial lake systems, it is slightly inclined (1%) towards a tributary of the Kalli River. The soil is Gleyic Luvisol. The thickness of the humus layer was 15–20 cm. The content of total carbon (TC), total

nitrogen (TN), nitrate (NO_3^--N), ammonia NH_4^+-N, Ca and Mg per dry matter in 10cm topsoil was 3.8 and 0.33 %, and 2.42, 2.89, 1487 and 283 mg kg^{-1}, respectively, which was correspondingly 6.3, 8.3, 4.4, 3.6, 2.3, and 2.0 times more than those in 20cm deep zone (Table S2).

The long-term average annual precipitation of the region is 650 mm, and the average temperature is 17.0 °C in July and –6.7 °C in January. The duration of the growing season is typically 175–180 days from mid-April to October[75].

The mean height of the forest stand is 17.5 m, the mean stem diameter at breast height 15.6 cm and the growing stock 245 m^3 ha^{-1} (based on Uri et al[76] and Becker et al[77]). In the forest floor, the following herbs dominate: *Filipendula ulmaria* (L.) Maxim., *Aegopodium podagraria* L., *Cirsium oleraceum* (L.) Scop., *Geum rivale* L., *Crepis paludosa* (L.) Moench,), shrubs (*Rubus idaeus* L., *Frangula alnus* L*., Daphne mezereum* L.) and young trees (*A. incana*, *Prunus padus* (L.)) dominate. In moss-layer *Climacium dendroides* (Hedw.) F. Weber & D. Mohr, *Plagiomnium* spp and *Rhytidiadelphus triquetrus* (Hedw.) Warnst.

5.2. Soil flux measurements

Soil fluxes were measured using 12 automatic dynamic chambers located close to each studied tree and installed in June 2017. The chambers were made from polymethyl methacrylate (Plexiglas) covered with non-transparent plastic film. Each soil chamber (volume of 0.032 m³) covered a 0.16 m² soil surface. To avoid stratification of gas inside the chamber, air with a constant flow rate of 1.8 L min^{-1} was circulated within a closed loop between the chamber and gas analyzer unit during the measurements by a diaphragm pump. The air sample was taken from the top of the chamber headspace and pumped back by distributing it to each side of the chamber. For the measurements, the soil chambers were closed automatically for 9 minutes each. Flushing time of the whole system with ambient air between measurement periods was 1 minute. Thus, there were approximately 12 measurements per chamber per day. A Picarro G2508 (Picarro Inc., Santa Clara, CA, USA) gas analyzer using cavity ring-down spectroscopy (CRDS) technology was used to monitor N_2O gas concentrations in the frequency of approximately 1.17 measurements per second. The chambers were connected to the gas analyzer using a multiplexer.

Since the 9 minutes of closing each soil chamber for measurements consisted of two minutes for stabilization the trend in the beginning and about two minutes unstable fluctuations at the end, for soil flux calculations, only 5 minutes of the linear trend of N_2O concentration change has been used for soil flux calculations.

After the quality checking 105,830 flux values (98.7% of total possible) of soil N_2O fluxes could be used during the whole study period.

5.3. Stem flux measurements

The tree stem fluxes were measured manually with frequency 1-2 times per week from September 2017 until December 2018. Twelve representative mature grey alder trees were selected for stem flux measurements and equipped with static closed tree stem chamber systems for stem flux measurements[49]. Soil fluxes were investigated close to each selected tree. The tree chambers were installed in June 2017 in following order: at the bottom part of the tree stem (approximately 10 cm above the soil) and at 80 and 170 cm above the ground. The rectangular shape stem chambers were made of transparent plastic containers, including removable airtight lids (Lock & Lock Co Ltd, Seoul, Republic of Korea). For chamber preparation see Schindler et al[28] .Two chambers per profile were set randomly across 180° and interconnected with tubes into one system (total volume of 0.00119 m³) covering 0.0108 m² of stem surface. A pump (model 1410VD, 12 V; Thomas GmbH, Fürstenfeldbruck, Germany) was used to homogenize the gas concentration prior to sampling. Chamber systems remained open between each sampling campaign. During 60 measurement campaigns, four gas samples (each 25 ml) were collected from each chamber system via septum in a 60 min interval: 0/60/120/180 min sequence (sampling time between 12:00 and 16:00) and stored in pre-evacuated (0.3 bar) 12 ml coated gas-tight vials (LabCo International, Ceregidion, UK). The gas samples were analysed in the laboratory at University of Tartu within a week using gas chromatograph (GC-2014; Shimadzu, Kyoto, Japan) equipped with an electron capture detector for detection of N_2O and a flame ionization detector for CH_4. The gas samples were injected automatically using Loftfield autosampler (Loftfield Analytics, Göttingen, Germany). For gas-chromatographical settings see Soosaar et al[24].

5.4. Soil and stem flux calculation

Fluxes were quantified on a linear approach according to change of CH_4 and N_2O concentrations in the chamber headspace over time, using the equation according to Livingston & Hutchison[78].

Stem fluxes were quantified on a linear approach according to change of N_2O concentrations in the chamber headspace over time. A data quality control was applied based on R^2 values of linear fit for CO_2 measurements. When the R^2 value for CO_2 efflux was above 0.9, the conditions inside the chamber were applicable, and the calculations for N_2O gases were also accepted in spite of their R^2 values.

To compare the contribution of soil and stems, the stem fluxes were upscaled to hectare of ground area based on average stem diameter, tree height, stem surface area, tree density, and stand basal area estimated for each period. A cylindric shape of tree stem was assumed. To estimate average stem emissions per tree, fitted regression curves for different periods were made between the stem emissions and height of the measurements as previously done by Schindler et al[32].

5.5. Eddy covariance instrumentation

Eddy-covariance system was installed on a 21 m height scaffolding tower. Fast 3-D sonic anemometer Gill HS-50 (Gill Instruments Ltd., Lymington, Hampshire, UK) was used to obtain 3 wind components. CO_2 fluxes were measured using the Li-Cor 7200 analyser (Li-Cor Inc., Lincoln, NE, USA). Air was sampled

synchronously with the 30 m teflon inlet tube and analyzed by a quantum cascade laser absorption spectrometer (QCLAS) (Aerodyne Research Inc., Billerica, MA, USA) for N_2O concentrations. The Aerodyne QCLAS was installed in the heated and ventilated cottage near the tower base. A high-capacity free scroll vacuum pump (Agilent, Santa Clara, CA, USA) guaranteed air flow rate 15 L min^{-1} between the tower and gas analyzer during the measurements. Air was filtered for dust and condense water. All measurements were done at 10Hz and the gas-analyzer reported concentrations per dry air (mixing ratios).

5.6. Eddy-covariance flux calculation and data quality control

The fluxes of N_2O were calculated using the EddyPro software (v.6.0-7.0, Li-Cor) as a covariance of the gas mixing ratio with the vertical wind component over 30-minute periods. Despiking of the raw data was performed following Mauder[79]. Anemometer tilt was corrected with the double axis rotation. Linear detrending was chosen over block averaging to minimize the influence of a possible fluctuations of a gas analyser. Time lags were detected using covariance maximisation in a given time window (5±2s was chosen based on the tube length and flow rate). While WPL-correction is typically performed for the closed-path systems, we did not apply it as water correction was already performed by the Aerodyne and the software reported mixing ratios. Both low and high frequency spectral corrections were applied using fully analytic corrections[80,81].

Calculated fluxes were filtered out in case they were coming from the half-hour averaging periods with at least one of the following criteria: more than 1000 spikes, half-hourly averaged mixing ratio out of range (300-350 ppb), quality control (QC) flags higher than 7^82.

Footprint area was estimated using Kljun et al[83] implemented in TOVI software (Li-Cor Inc.). Footprint allocation tool was implemented to flag the non-forested areas within the 90% cumulative footprint and fluxes appointed to these areas were removed from the further analysis.

Storage fluxes were estimated using point concentration measurements from the eddy system, assuming the uniform change within the air column under the tower during every 30 min period (calculated in EddyPro software). In the absence of a better estimate or profile measurements, these estimates were used to correct for storage change. Total flux values that were higher than eight times the standard deviation were additionally filtered out (following Wang et al., 2013[84]). Overall, the quality control procedures resulted in 61% data coverage.

While friction velocity (u*) threshold is used to filter eddy fluxes of CO_2[85], visual inspection of the friction velocity influence on N_2O fluxes demonstrated no effect. Thus, we decided not to apply it, taking into account that 1-9 QC flag system already marks the times when the turbulence is not sufficient.

To obtain the continuous time-series and to enable the comparison to chamber estimates over hourly time scales, gap-filling of N_2O fluxes was performed using marginal distribution sampling method

implemented in ReddyProcWeb online tool (https://www.bgc-jena.mpg.de/bgi/index.php/Services/REddyProcWeb) (described in detail in Wutzler et al[86].

MATLAB (ver. 2018a-b, Mathworks Inc., Natick, MA, USA) was used for all the eddy fluxes data analysis.

5.7. Ancillary measurements

Air temperature and relative humidity were measured within the canopy at 10m height using the HC2A-S3 – Standard Meteo Probe / RS24T (Rotronic AG, Bassersdorf, Switzerland) and Campbell CR100 data logger (Campbell Scientific Inc., Logan, UT, USA). Based on these data, dew point depression was calculated to characterise chance of fog formation within the canopy. The incoming solar radiation data were obtained from the SMEAR Estonia station located at 2 km from the study site[87] using the Delta-T-SPN-1 sunshine pyranometer (Delta-T Devices Ltd., Cambridge, UK). The cloudiness ratio was calculated based on radiation data.

Near-ground air temperature, soil temperature (Campbell Scientific Inc.) and soil water content sensors (ML3 ThetaProbe, Delta-T Devices, Burwell, Cambridge, UK) were installed directly on the ground and 0–10 cm soil depth close to the studied tree spots. During six campaigns from August to November 2017 composite topsoil samples were taken with a soil corer from a depth of 0–10 cm for physical and chemical analysis using standard methods[88].

5.8. Statistical analysis

R version 4.0.2 (R Development Core Team, 2020) was used to examine, analyse and visualise the data. The significance level (alpha) considered for all the tests was 0.05. The “akima” package version 0.6-2.1 was used to create interpolated contour plots representing a three-dimensional surface[89] by plotting soil temperature and SWC against soil N_2O emissions as the independent variable. Linear regression models were fitted for change of SWC and soil N_2O flux in period Drought onset and air temperature and soil N_2O flux in period Freeze–Thaw. Regarding all measurements of soil temperature, SWC and soil N_2O flux, relationships were better represented by nonlinear than linear models. In addition, Bragg equation with four parameters[90] was used for describing relationship between SWC and soil N_2O flux in period Dry. A workflow for the nonlinear regression analysis was used[91] and regression models were fitted in R using functions lm, nls or loess.

Declarations

Acknowledgements

This study was supported by the Ministry of Education and Science of Estonia (SF0180127s08 grant), the Estonian Research Council (IUT2-16, PRG-352, and MOBERC20), the Czech Science Foundation (17-18112Y) and project SustES - Adaptation strategies for sustainable ecosystem services and food security under adverse environmental conditions (CZ.02.1.01/0.0/0.0/16_019/0000797), the EU through the

European Regional Development Fund (Centres of Excellence ENVIRON, grant number TK-107, EcolChange, grant number TK-131, and the MOBTP101 returning researcher grant by the Mobilitas Pluss programme) and the European Social Fund (Doctoral School of Earth Sciences and Ecology). This work was also supported by Academy of Finland (294088, 288494), and from the European Research Council (ERC) under the European Union's Horizon 2020 research and innovation programme under grant agreement No [757695]. We would like to thank Marek Jakubík for his technical support.

Contributions

Ü.M., K.S., K.M. and Ü.N. designed this study, Ü.M., K.S., A.K., J.P., M.E., J.E.G., T.S., M.P and P.M. wrote the paper, T.S., M.M., K.S. and Ü.M. conducted the field work, Ü.M., K.S., A.K., M.E., J.E.G and K.M. carried out data checks and analysis, J.P. deposited the data, and all authors commented on the paper.

Competing interests

The authors declare no competing interests.

Additional information

Supplementary information is available for this paper at …….

References

1. Baldocchi, D. Measuring fluxes of trace gases and energy between ecosystems and the atmosphere - the state and future of the eddy covariance method. *Glob. Chang. Biol*. 3600–3609 (2014). https://doi.org/10.1111/gcb.12649.
2. U.S. EPA. *Methane and nitrous oxide emissions from natural sources*. EPA 430-R-10- 001 (2010).
3. Myhre, G. et al. Anthropogenic and natural radiative forcing. In: *Climate change 2013: The physical science basis. Working Group I contribution to the Fifth Assessment Report of the Intergovernmental Panel on Climate Change*. Cambridge Univ. Press, Cambridge, UK. p. 659–740 (2013)
4. Saikawa, E. et al. Global and regional emissions estimates for N_2O. *Atmos. Chem. Phys*. 14, 4617–4641 (2014).
5. Ravishankara, A.R., Daniel, J.S. & Portmann, R.W. Nitrous oxide (N_2O): The dominant ozone depleting substance emitted in the 21st century. *Science* 326, 123-125 (2009).
6. Riis, T. et al. Global overview of ecosystem services provided by riparian vegetation. *BioScience* 70, 6, 501–514 (2020).
7. Mander, Ü., Tournebize, J., Tonderski, K., Verhoeven, J.T.A. & Mitsch, J.W. Planning and establishment principles for constructed wetlands and riparian buffer zones in agricultural catchments. *Ecol. Eng*. 103, 296-300 (2017).
8. Sweeney, B.W. et al. Riparian deforestation, stream narrowing, and loss of stream ecosystem services. *Proc. Natl. Acad. Sci. U.S.A.* 101, 14132–14137 (2004).

9. 9. Groh, T.A., Davis, M.P., Isenhart, T.M., Jaynes, D.B. & Parkin, T.B. In situ denitrification in saturated riparian buffers. *Environ. Qual*. 48, 376–384 (2019).
10. Butterbach-Bahl, K., Baggs, E. M., Dannenmann, M., Kiese, R. & Zechmeister-Boltenstern, S. Nitrous oxide emissions from soils: How well do we understand the processes and their controls? *Philos. Trans. R. Soc. B Biol. Sci*. 368, (2013).
11. Mander, Ü. et al. Isotopologue ratios of N_2O and N_2 measurements underpin the importance of denitrification in differently N-loaded riparian alder forests. *Environ. Sci. Technol*. 48, 20, 11910-11918 (2014).
12. Uri, V. et al. Long-term effects on the nitrogen budget of a short-rotation grey alder (*Alnus incana* (L.) Moench) forest on abandoned agricultural land. *Ecol. Eng*. 37(6), 920-930 (2011).
13. Binkley, D., Sollins, P., Bell, R., Sachs, D. & Myrold, D. Biogeochemistry of adjacent conifer and alder-conifer stands. *Ecology* 73, 6, 2022–2033 (1992).
14. Caudullo, G., Welk, E., San-Miguel-Ayanz, J. Chorological maps for the main European woody species. *Data in Brief* 12, 662-666 (2017).
15. Clerici, N., Weissteiner, C.J., Paracchini, M.L., Boschetti, L., Baraldi, A. & Strobl, P. Pan-European distribution modelling of stream riparian zones based on multi-source Earth Observation data. *Ecol. Indic.* 24, 211–223 (2013).
16. Pihlatie, M. et al. Nitrous oxide emissions from a beech forest floor measured by eddy covariance and soil enclosure techniques. *Biogeosciences* 2, 377–387 (2005).
17. Von Arnold, K., Weslien, P., Nilsson, M., Svensson, B.H. & Klemedtsson, L. Fluxes of CO_2, CH_4 and N_2O from drained coniferous forests on organic soils. *Forest Ecol. Manage*. 210, 239–254 (2005).
18. Pilegaard, K. et al. Factors controlling regional differences in forest soil emission of nitrogen oxides (NO and N_2O). *Biogeosciences* 3, 651–661 (2006).
19. Savage, K., Phillips, R. & Davidson, E. High temporal frequency measurements of greenhouse gas emissions from soils. *Biogeosciences* 11, 2709–2720 (2014).
20. Wu, B. & Mu, C.C. Effects on greenhouse gas (CH_4, CO_2, N_2O) emissions of conversion from over-mature forest to secondary forest and Korean Pine plantation in Northeast China. *Forests* 10, 788 (2019).
21. Dalal, R.C. & Allen, D.E. Greenhouse gas fluxes from natural ecosystems. *Aust. J. Bot.* 56, 369 (2008).
22. DeSimone, J., Macrae, M.L. & Bourbonniere, R.A. Spatial variability in surface N_2O fluxes across a riparian zone and relationships with soil environmental conditions and nutrient supply. *Agr. Ecosyst. Environ*. 138, 1–9 (2010).
23. Hefting, M.M., Bobbink, R., & de Caluwe, H. Nitrous oxide emission and denitrification in chronically nitrate-loaded riparian buffer zones. *J. Environ. Qual*. 32, 1194–1203 (2003).
24. Soosaar, K. et al. Dynamics of gaseous nitrogen and carbon fluxes in riparian alder forests. *Ecol. Eng*. 37, 40–53 (2011).

25. Liu, X.P., Zhang, W.J., Hu, C.S., & Tang, X.G. Soil greenhouse gas fluxes from different tree species on Taihang Mountain, North China. *Biogeosciences* 11, 6, 1649–1666 (2014).
26. Mander, Ü. et al. The impact of a pulsing groundwater table on greenhouse gas emissions in riparian grey alder stands. *Environ. Sci. Pollut. Res*. 22, 2360-2371 (2015).
27. De Carlo, N.D., Oelbermann, M., & Gordon, A.M. Spatial and temporal variation in soil nitrous oxide emissions from a rehabilitated and undisturbed riparian forest. *J. Environ. Qual*. 48, 624–633 (2019).
28. Schindler, T. et al. Short-term flooding increases CH_4 and N_2O emissions from trees in a riparian forest soil-stem continuum. *Sci. Rep.* 10, 1, 3204 (2020).
29. Pihlatie et al Greenhouse gas fluxes in a drained peatland forest during spring frost-thaw event. *Biogeosciences* 7, 1715–1727 (2010).
30. Hagedorn, F. & Bellamy, P. Hot spots and hot moments for greenhouse gas emissions from soils. In Robert Jandl, E., Rodeghiero M. & Olsson, M. (eds) *Soil Carbon in Sensitive European Ecosystems: From Science to Land Management*. Blackwell Science Publ., Oxford, UK, pp. 13-32 (2011).
31. Christiansen, J.R., Vesterdal, L. & Gundersen, P. Nitrous oxide and methane exchange in two small temperate forest catchments - effects of hydrological gradients and implications for global warming potentials of forest soils. *Biogeochemistry* 107, 437–454 (2012).
32. Pärn, J. et al. Nitrogen-rich organic soils under warm well-drained conditions are global nitrous oxide emission hotspots. *Nat. Commun*. 9, 1–8 (2018).
33. Liengaard, L. et al. Hot moments of N_2O transformation and emission in tropical soils from the Pantanal and the Amazon (Brazil). *Soil Biol. Biochem*. 75, 26-36 (2014).
34. Almaraz, M., Groffman, P. M., & Porder, S. Effects of changes in nitrogen availability on nitrogen gas emissions in a tropical forest during a drought. *J. Geophys. Res. Biogeosciences* 124, 2917–2926 (2019).
35. Muhr, J., Goldberg, S.D., Borken, W. & Gebauer, G. Repeated drying–rewetting cycles and their effects on the emission of CO_2, N_2O, NO, and CH_4 in a forest soil. *J. Plant Nutr. Soil Sci*. 171, 719–728 (2008).
36. Goldberg, S.D. & Gebauer, G. N_2O and NO fluxes between a Norway spruce forest soil and atmosphere as affected by prolonged summer drought. *Soil Biol. Biochem*. 41, 1986–1995 (2009)
37. Shrestha, N.K. & Wang, J.Y. Current and future hot-spots and hot-moments of nitrous oxide emission in a cold climate river basin. *Environ. Pollut*. 239, 648-660 (2018)
38. Welch, B., Gauci, V., Sayer, E.J. Tree stem bases are sources of CH_4 and N_2O in a tropical forest on upland soil during the dry to wet season transition. Global Change Biology 25, 361–372 (2019).
39. Teepe, R., Brumme, R. & Beese, F. Nitrous oxide emissions from frozen soils under agricultural, fallow and forest land. *Soil Biol. Biochem*. 32, 1807-1810 (2000).
40. Chen, L.X., Chen; Z.S., Jia, G.D., Zhou, J., Zhao, J.C. & Zhang, Z.Q. Influences of forest cover on soil Freeze–Thaw dynamics and greenhouse gas emissions through the regulation of snow regimes: A comparison study of the farmland and forest plantation. *Sci. Total Environ*. 726, 138403 (2020).

41. Teepe, R., Vor, A., Beese, F. & Ludwig, B. Emissions of N_2O from soils during cycles of freezing and thawing and the effects of soil water, texture and duration of freezing. *Eur. J. Soil Sci*. 55, 2, 357–365 (2004).
42. Viru, B. et al. Wintertime greenhouse gas fluxes from hemiboreal drained peatlands. *Atmosphere* 11, 731 (2020).
43. Groffman, P., Hardy, J., Driscoll, C.T. & Fahey, T.J. Snow depth, soil freezing, and fluxes of carbon dioxide, nitrous oxide and methane in a northern hardwood forest. *Glob. Change Biol*. 12, 1748–1760 (2006).
44. Teepe, R., Brumme, R., Beese, F. Nitrous oxide emissions from soil during freezing and thawing periods. *Soil Biol. Biochem*. 33, 1269–1275 (2001).
45. Groffman, P.M., Driscoll, C.T., Fahey, T.J., Hardy, J.P., Fitzhugh, R.D., Tierney, G.L. Colder soils in a warmer world: a snow manipulation study in a northern hardwood forest ecosystem. Biogeochemistry 56, 2, 135–150 (2001).
46. Rusch, H. & Rennenberg, H. Black alder (*Alnus glutinosa* (L.) Gaertn.) trees mediate methane and nitrous oxide emission from the soil to the atmosphere. *Plant Soil* 201, 1–7 (1998).
47. Machacova, K., Papen, H., Kreuzwieser, J. & Rennenberg, H. Inundation strongly stimulates nitrous oxide emissions from stems of the upland tree *Fagus sylvatica* and the riparian tree *Alnus glutinosa*. *Plant Soil* 364, 287–301 (2013).
48. Liu, X. P., Zhang, W. J., Hu, C. S., & Tang, X. G. Soil greenhouse gas fluxes from different tree species on Taihang Mountain, North China. *Biogeosciences* 11, 6, 1649–1666 (2014).
49. Machacova, K. et al. *Pinus sylvestris* as a missing source of nitrous oxide and methane in boreal forest. *Sci. Rep*. 6, 1–8 (2016).
50. Wen, Y., Corre, M.D., Rachow, C., Chen, L., Veldkamp, E. Nitrous oxide emissions from stems of alder, beech and spruce in a temperate forest. *Plant Soil* 420, 423–434 (2017).
51. Machacova, K., Vainio, E., Urban, O. & Pihlatie, M. Seasonal dynamics of stem N_2O exchange follow the physiological activity of boreal trees. *Nat. Commun*. 10, 1–13 (2019).
52. Ward, N.D., Indivero, J., Gunn, C., Wang, W., Bailey, V. & McDowell, N.G. Longitudinal gradients in tree stem greenhouse gas concentrations across six Pacific Northwest coastal forests. *J. Geophys. Res. Biogeosci.* 124, 6, 1401-1412 (2019).
53. Barba, J., Poyatos, R. & Vargas, R. Automated measurements of greenhouse gases fluxes from tree stems and soils: magnitudes, patterns and drivers. *Sci. Rep*. 9, 4005 (2019).
54. Vargas, R. & Barba, J. Greenhouse Gas Fluxes From Tree Stems. *Trends Plant Sci*. 24, 296–299 (2019).
55. Eugster, W., Zeyer, K., Zeeman, M., Michna, P., Zingg, A., Buchmann, N. & Emmenegger, L. Methodical study of nitrous oxide eddy covariance measurements using quantum cascade laser spectrometry over a Swiss forest. *Biogeosciences* 4, 927-939 (2007).

56. Nemitz, E. et al. Standardisation of eddy-covariance flux measurements of methane and nitrous oxide. *Int. Agrophys*. 32, 517-549 (2018).
57. Weitzman, J.N. & Kaye, J.P. Nitrogen budget and topographic controls on nitrous oxide in a shale-based watershed. *J. Geophys. Res. Biogeosci.* 123, 1888–1908 (2018).
58. Barrat, H.A., Evans, J., Chadwick, D.R., Clark, I.M., Le Cocq, K. & Cardenas, L.M. The impact of drought and rewetting on N_2O emissions from soil in temperate and Mediterranean climates. *Eur. J. Soil Sci*. 1-13 (2020). doi: 10.1111/ejss.13015.
59. McDaniel, M.D., Kaye, J.P. & Kaye, M.W. Do “hot moments” become hotter under climate change? Soil nitrogen dynamics from a climate manipulation experiment in a post-harvest forest. *Biogeochemistry* 121, 339–354 (2014).
60. Petrakis, S., Seyfferth, A., Kan, J.J., Inamdar, S. & Vargas, R. Influence of experimental extreme water pulses on greenhouse gas emissions from soils. *Biogeochemistry* 133, 147–164 (2017).
61. Kim, D.-G., Vargas, R., Bond-Lamberty, B. & Turetsky, M.R. Effects of soil rewetting and thawing on soil gas fluxes: a review of current literature and suggestions for future research. *Biogeosciences* 9, 2459-2483 (2012).
62. Wagner-Riddle, C. et al. Globally important nitrous oxide emissions from croplands induced by freeze–thaw cycles. *Nat. Geosci*. 10, 279–283 (2017).
63. Tian et al. The global N_2O model intercomparison project. *B. Am. Meteorol. Soc*. 99, 6, 1231-1252 (2018).
64. Öquist, M.G. et al. Nitrous oxide production in a forest soil at low temperatures –processes and environmental controls. *FEMS Microbiol. Ecol*. 49, 371–378 (2004).
65. Matzner, E. & Borken, W. Do freeze–thaw events enhance C and N losses from soils of different ecosystems? A review. *Eur. J. Soil Sci*. 59, 2, 274-284 (2008).
66. Bateman, E. J. & Baggs, E. M. Contributions of nitrification and denitrification to N_2O emissions from soils at different water-filled pore space. *Biol. Fertil. Soils* 41, 379–388 (2005).
67. Li et al. Terrestrial N_2O emissions and related functional genes under climate change: A global meta-analysis. *Glob. Change Biol*. 26, 931–943 (2020).
68. Sinha, V. et al. OH reactivity measurements within a boreal forest: Evidence for unknown reactive emissions. *Environ. Sci. Technol*. 44, 6614–6620 (2010).
69. Martinez, M. et al. Hydroxyl radicals in the tropical troposphere over the Suriname rainforest: airborne measurements. Atmos. Chem. Phys. 10, 3759–3773 (2010).
70. Dowdell, R.J., Burford, J.R. & Crees, R. Losses of nitrous oxide dissolved in drainage water from agricultural land. *Nature* 278, 342–343 (1979).
71. Warneke, S., Macdonald, B.C.T., Macdonald,L.M., Sanderman, J. & Farrell, M. 2015. Abiotic dissolution and biological uptake of nitrous oxide in Mediterranean woodland and pasture soil. *Soil Biol. Biochem*. 82, 62-64 (2015).

72. Min, K.-E., Pusede, S.E., Browne, E.C., LaFranchi, B.W., Wooldridge, P.J. & Cohen, R.C. Eddy covariance fluxes and vertical concentration gradient measurements of NO and NO_2 over a ponderosa pine ecosystem: observational evidence for within-canopy chemical removal of NOx. *Atmos. Chem. Phys*. 14, 5495–5512 (2014).
73. Fulgham, S.R., Millet, D.B., Alwe, H.D., Goldstein, A.H., Schobesberger, S. & Farmer, D.K. Surface wetness as an unexpected control on forest exchange of volatile organic acids. *Geophys. Res. Lett*. 47, e2020GL088745, (2020).
74. Varep, E. The landscape regions of Estonia. Publications on Geography IV. *Acta et Comm. Universitatis Tartuensis* 156, 3–28 (1964).
75. Kupper, P. et al. An experimental facility for free air humidity manipulation (FAHM) can alter water flux through deciduous tree canopy. *Environ. Exp. Bot.* 72, 432–438 (2011).
76. Uri, V. et al. The dynamics of biomass production, carbon and nitrogen accumulation in grey alder (*Alnus incana* (L.) Moench) chronosequence stands in Estonia. *Forest Ecol. Manag*. 327, 106-117 (2014).
77. Becker, H. et al. The effects of clear-cut on net nitrogen mineralization and nitrogen losses in a grey alder stand. Ecol. Engi. 85, 237-246 (2015).
78. Livingston, G. P. & Hutchinson, G. L. Enclosure-based measurement of trace gas exchange: Applications and sources of error. in *Biogenic Trace Gases: Measuring Emissions from Soil and Water* (eds. Matson, P.A. & Harriss, R.C.) 14–51 (Ed. Blackwell Publishing: Oxford, UK (1995).
79. Mauder, M. et al. A strategy for quality and uncertainty assessment of long-term eddy-covariance measurements. *Agr. Forest Meteorol*. 169, 122-135. (2013).
80. Moncrieff, J. B. et al. A system to measure surface fluxes of momentum, sensible heat, water vapor and carbon dioxide. *J. Hydrol*. 188-189, 589-611 (1997).
81. Moncrieff, J.B., Clement, R. Finnigan, J. & Meyers T. Averaging, detrending and filtering of eddy covariance time series. in *Handbook of Micrometeorology: A Guide for Surface Flux Measurements*, Lee, X., W. J. Massman & Law, B.E., Eds. Dordrecht: Kluwer Academic, 7-31 (2004).
82. Foken, T., Göockede, M., & Mauder, M. Post-field data quality control. in *Handbook of Micrometeorology: a Guide for Surface Flux Analysis*. (Lee, X.H., Massman, W. & Law, B., Eds.) Issue 1988, pp181–208. (2004).
83. Kljun, N., Calanca, P., Rotach, M.W. & Schmid, H.P. A Simple Two-dimensional Parameterisation for Flux Footprint Prediction (FFP). *Geosci. Model Dev.* 3695–3713 (2015).
84. Wang, J. M., Murphy, J. G., Geddes, J. A., Winsborough, C. L., Basiliko, N. & Thomas, S. C. Methane fluxes measured by eddy covariance and static chamber techniques at a temperate forest in central Ontario, Canada. Biogeosciences, 10, 6, 4371-4382 (2013).
85. Papale, D. et al. Towards a standardized processing of Net Ecosystem Exchange measured with eddy covariance technique: algorithms and uncertainty estimation. *Biogeosciences* 3, 4, 571–583 (2006).

86. Wutzler, T. et al. Basic and extensible post-processing of eddy covariance flux data with REddyProc. *Biogeosciences Discussions* 1–39. (2018).
87. Noe, S.M. et al. SMEAR Estonia: Perspectives of a large-scale ecosystem-atmosphere research infrastructure. *Forestry Studies* 63, 66-84 (2015).
88. APHA-AWWA-WEF. *Standard Methods for the Examination of Water and Wastewater*, 21th ed. American Public Health Organisation (2005).
89. Akima, H., Gebhardt, A., Petzold, T., & Maechler, M. akima: Interpolation of irregularly and regularly spaced data. R Package Version 0.6-2.1. (2016). https://cran.r-project.org/web/packages/akima/index.html (accessed 06.08.2020)
90. Ratkwosky, D. A. Handbook of Nonlinear Regression Models (No. 04; QA278. 2, R3.). M. Dekker, New York, USA, 241 p. (1990).
91. .Archontoulis, S.V. & Miguez, F.E. Nonlinear regression models and applications in agricultural research. *Agron. J.* 107, 2, 786-798 (2015).

Tables

Table 1. Fluxes of N_2O from all the sources during the study period: September 2017 – December 2019 for the soil and ecosystem, September 2017 – December 2018 for stems. EC – eddy covariance.

Source	Period	N_2O flux	
		mg N m^{-2}-period^{-1}	%
Soil	Wet	59.9	13.1
	Dry	104.9	22.9
	Freeze–Thaw	64.9	14.1
	Dry-minor	26.4	5.8
	Other	202.7	44.1
	Total	**458.8**	100.0
Stems	Wet	1.44	40.7
	Dry	0.41	11.7
	Other	1.68	47.6
	Total	**3.53**	100.0
Ecosystem (EC)	Wet	17.3	19.8
	Dry	2.26	2.6
	Freeze–Thaw	1.96	2.3
	Dry-minor	0.48	0.6
	Other	65.3	74.7
	Total	**87.3**	100.0

Figures

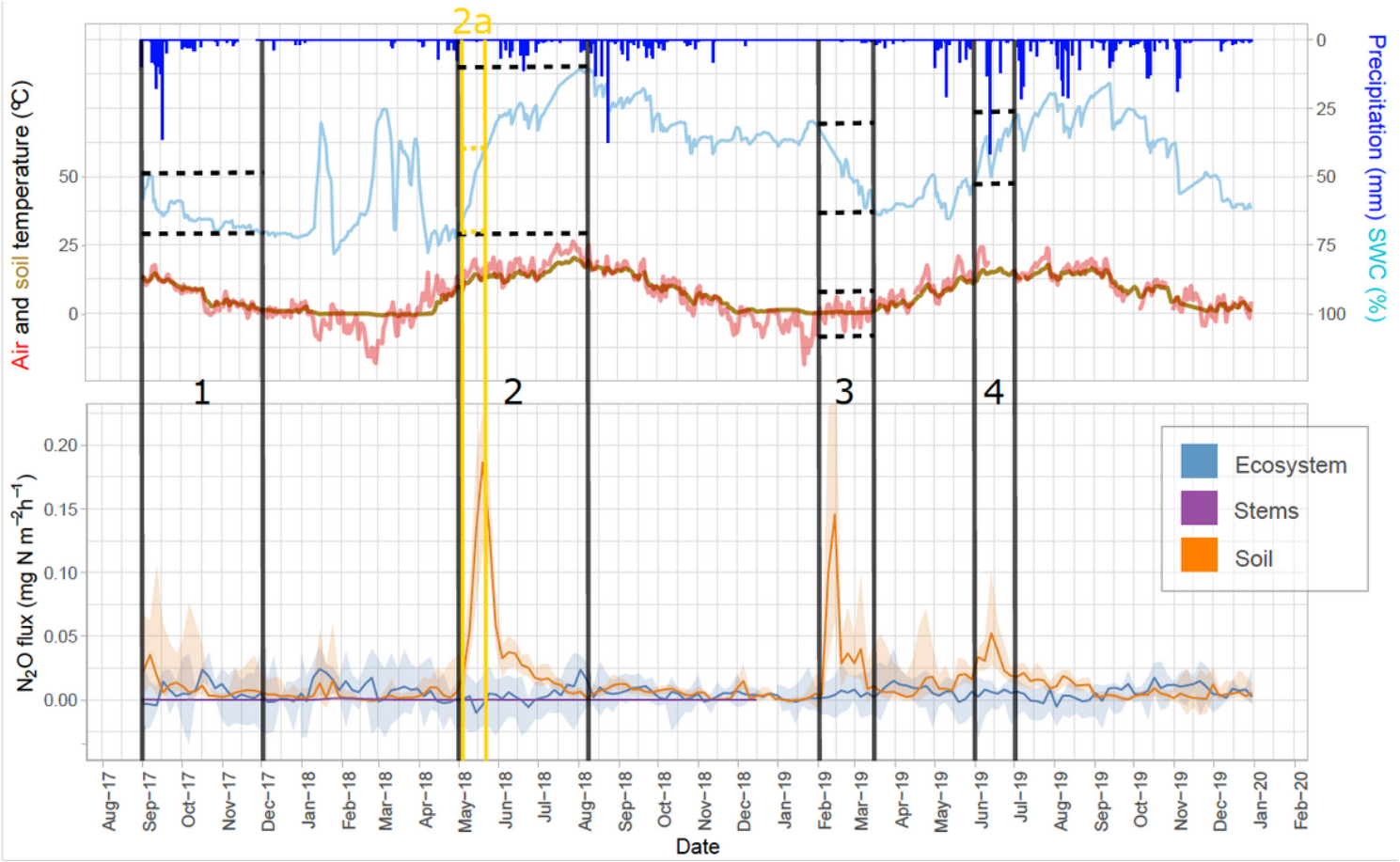

Figure 1

Dynamics of ecosystem-level N2O fluxes in the Agali grey alder forest during the study period September 2017 – December 2019. Lines – 5-days median values, shaded area - 25th and 75th percentiles. Vertical lines show start and end of hot moments: 1 – Wet (2017-09-01 … 2017-12-01), 2 – Dry (2018-05-01 … 2018-08-05) with 2a -Drought Onset (2018-05-02 … 2018-05-21), 3 – Freeze–Thaw (2019-02-01 … 2019-03-15), and 4 – Dry-minor (2019-02-01 … 2019-03-15). Horizontal dashed lines mark the range of soil water content during the hot moments and near-ground air temperature for Freeze–Thaw period. SWC – soil water content).

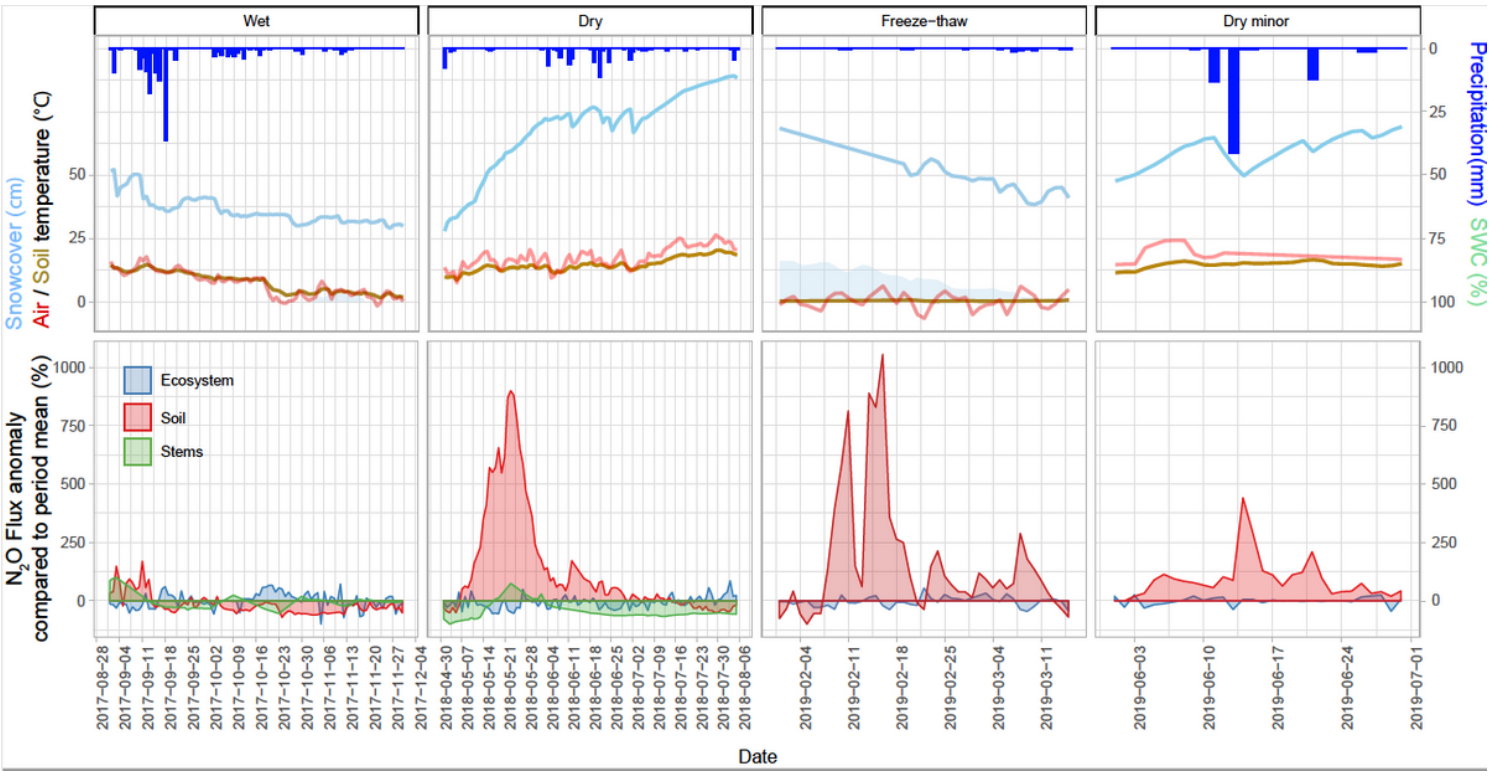

Figure 2

The Wet, Dry, Freeze–Thaw and Dry-minor hot moments of N2O emissions at ecosystem, tree stem and soil level in the Agali grey alder forest. The Drought Onset phase of Dry period is marked with the peaking N2O flux on 2018-05-20. The flux values are presented in relative units – percentage of change compared to the mean flux of the full period.

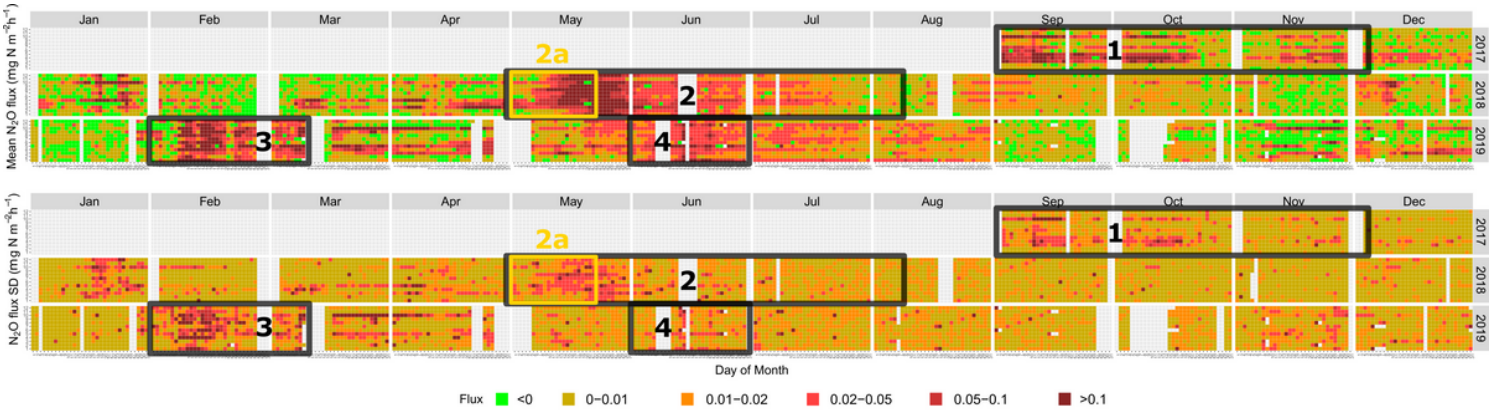

Figure 3

Heatmap of N2O soil fluxes (mg N2O-N m-2 h-1) showing chamber-based spatial-temporal dynamics of the whole study period (2017-01-09…2019-12-31). Value of each chamber (1-12 down–top in each year-bar) is averaged from all measurements during a given day after quality check (max. 12 measurements per day). (a) Daily average values of N2O soil flux per chamber. (b) Standard deviation values of N2O soil

flux per chamber. Hot moments: 1 – Wet, 2 – Dry with Drought Onset (2a), 3 – Freeze–Thaw, 4 – Dry-minor.

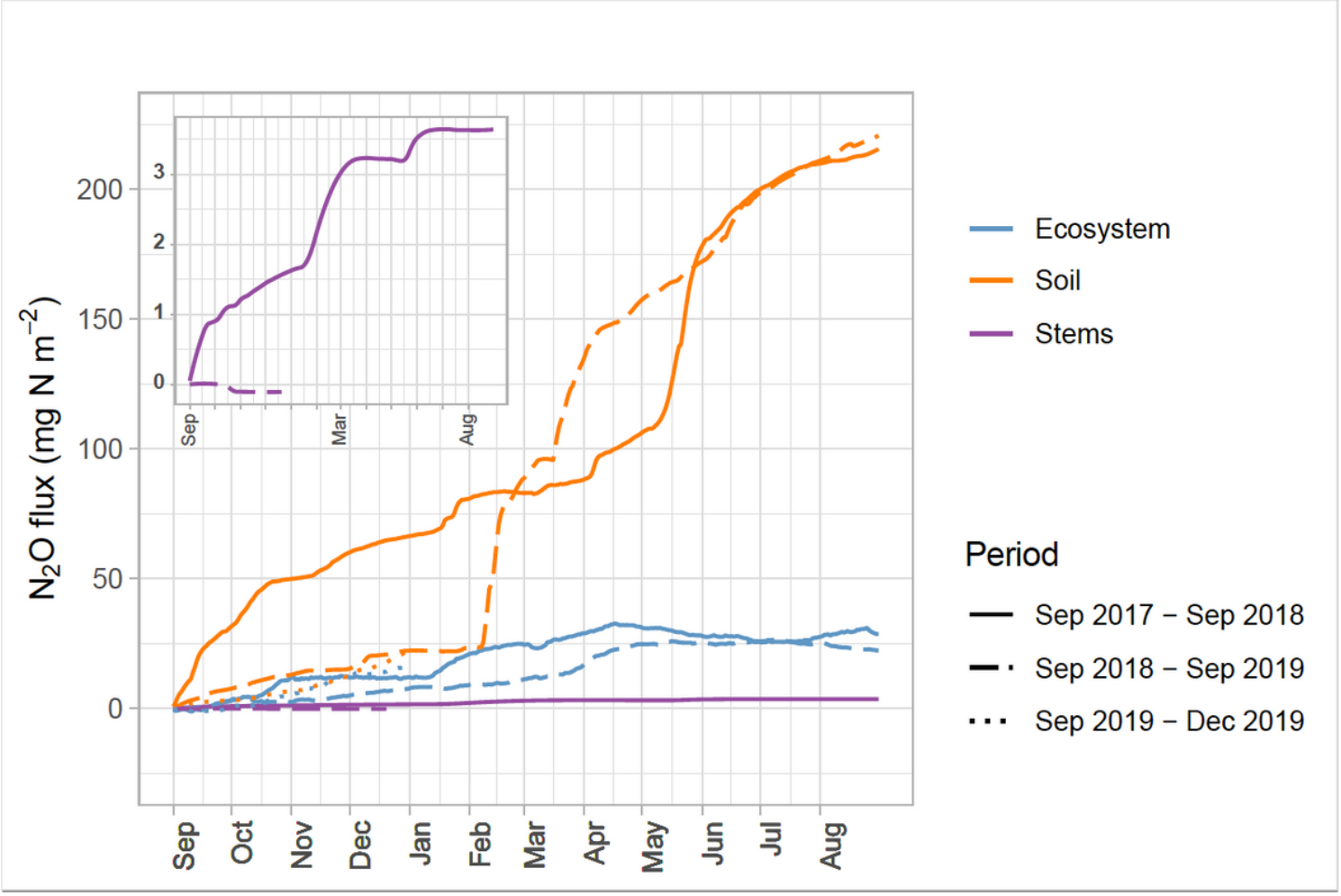

Figure 4

Cumulative fluxes of N2O from soil, stems and ecosystem (eddy covariance above the canopies) during two full years (Sept. 2017 –Sept. 2019) and one half-year (Sept. – Dec. 2019). Due to significantly lower values, the stem fluxes are zoomed in. Notice that the stem fluxes have been measured from Sept. 2017 to Dec. 2018.

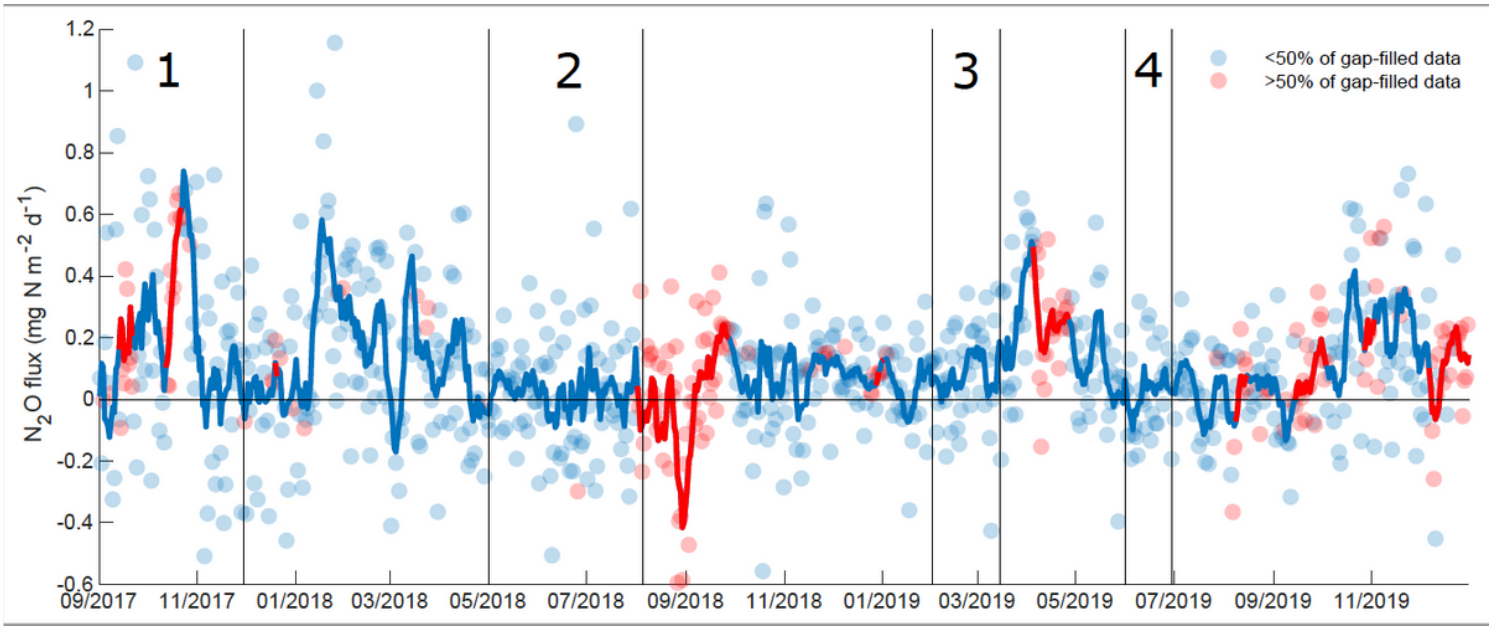

Figure 5

Seasonal cycle of ecosystem N2O flux measured with QCLAS in eddy tower. The markers denote daily total values, the line is a 7-day running mean. The periods marked with red color represent time intervals with gap-filled data (MDS-method) exceeding 50%. Hot moments: 1 – Wet, 2 – Drought (without showing Drought Onset), 3 – Freeze–Thaw and 4 – Dry-minor.

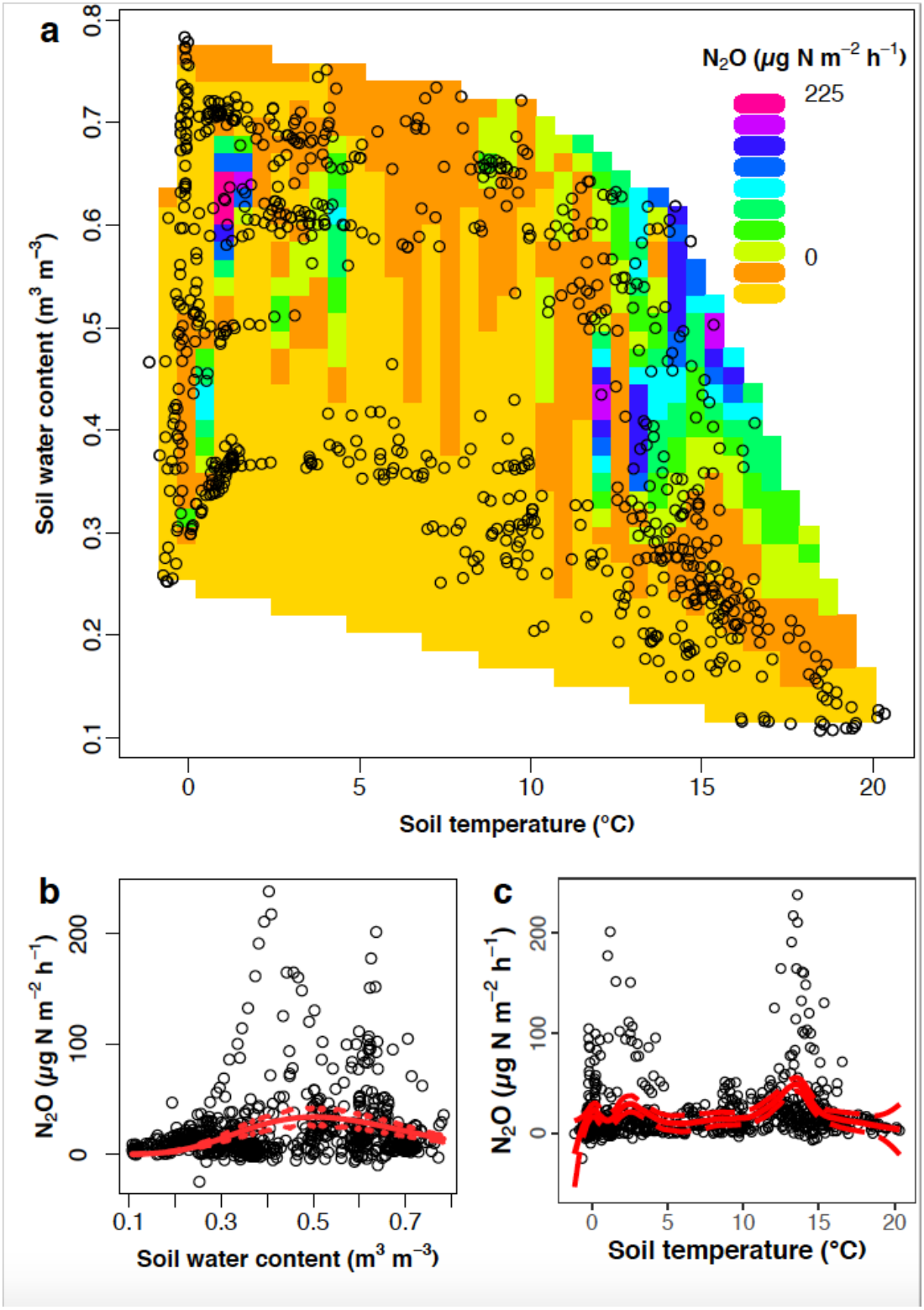

Figure 6

Relationships between the soil temperature, soil water content (SWC) and flux of N2O from soil over the whole study period. (a) Contour plot showing relationships between soil temperature, SWC and N2O emission (n = 755). (b) Regression curve of SWC vs N2O fluxes. Curve fitted regression of SWC and N2O flux (R2 = 0.07, p < 0.01, n = 757). N2O = (15725.05 × SWC7.73) × exp(−15.38 × SWC). (c) Regression

curve of soil temperature vs N2O. Local polynomial regression fitting of soil temperature and N2O flux (R2 = 0.13, p < 0.01, n = 756). The dashed red lines represent 95% confidence intervals for the regression line.

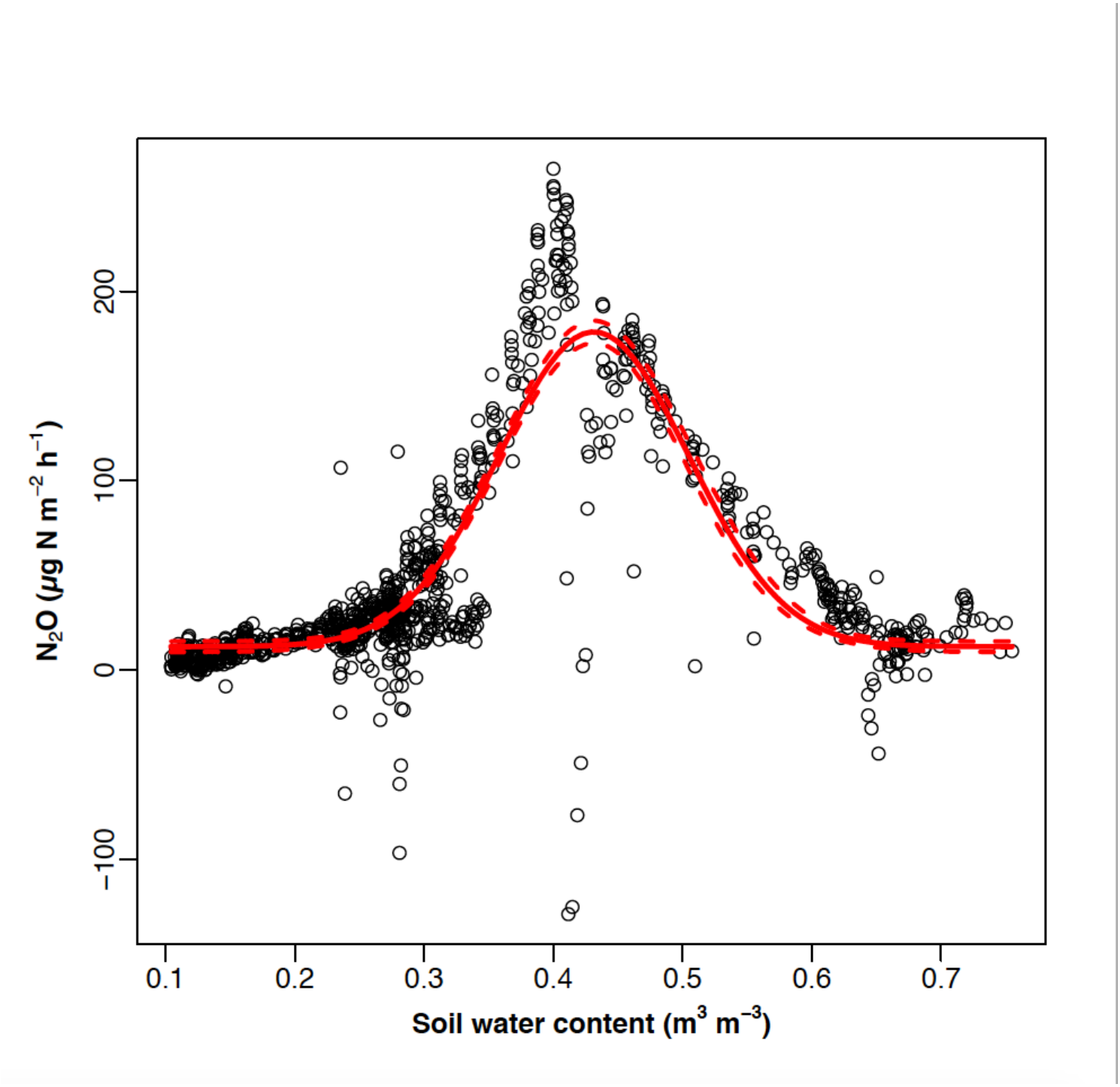

Figure 7

Dynamics of soil water content (SWC) vs soil N2O flux (hourly average values) during the hot moment Dry (2018-05-01 … 2018-08-05). The curve is calculated after the Bragg equation with four parameters: Y = c + (d − c) × exp(−b × (X − e)2, where b = 92.77, c = 0.0123, d = 0.1786, e = 0.4314 and X is SWC and Y is N2O flux (R2 = 0.74, p < 0.001, n = 1065).

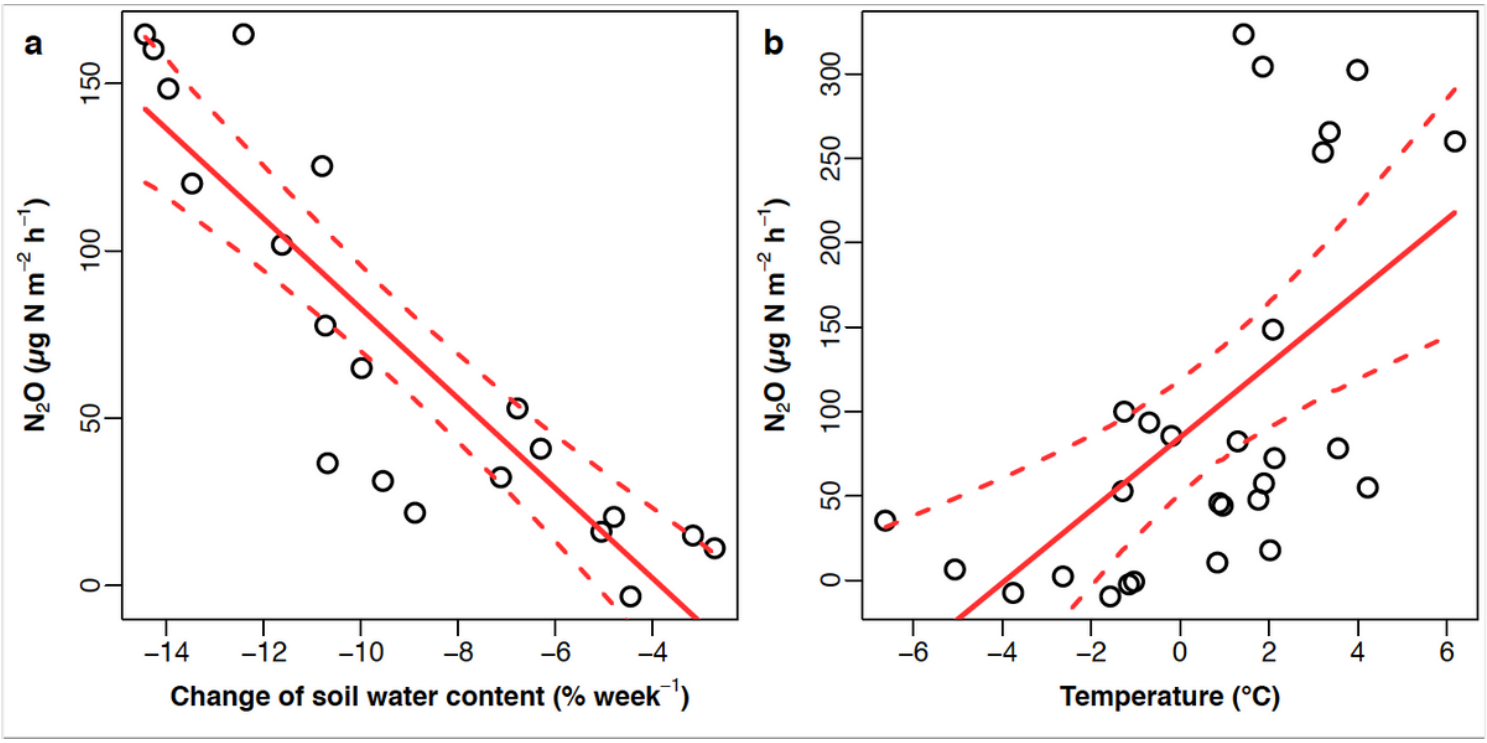

Figure 8

Main determinants of N2O soil fluxes differ between the hot moments. (a) During the beginning of Dry period (Drought Onset; 2018-05-02 to 2018-05-21) the speed of decrease in soil moisture determines the N2O flux increase. The linear fitted regression of change of soil moisture (CSM) and N2O flux (R2 = 0.78, $p < 0.01$, n = 20). N2O = −0.0517 + (−0.0134) × CSM. (b) During the Freeze–Thaw period (2019-02-01 to 2019-03-15) N2O flux is correlated with air temperature (Tair) (R2 = 0.30, $p < 0.001$, n = 41). N2O = 0.0819 + (0.0173) × Tair. On both figures, the dashed red lines represent 95% confidence intervals for the regression line.

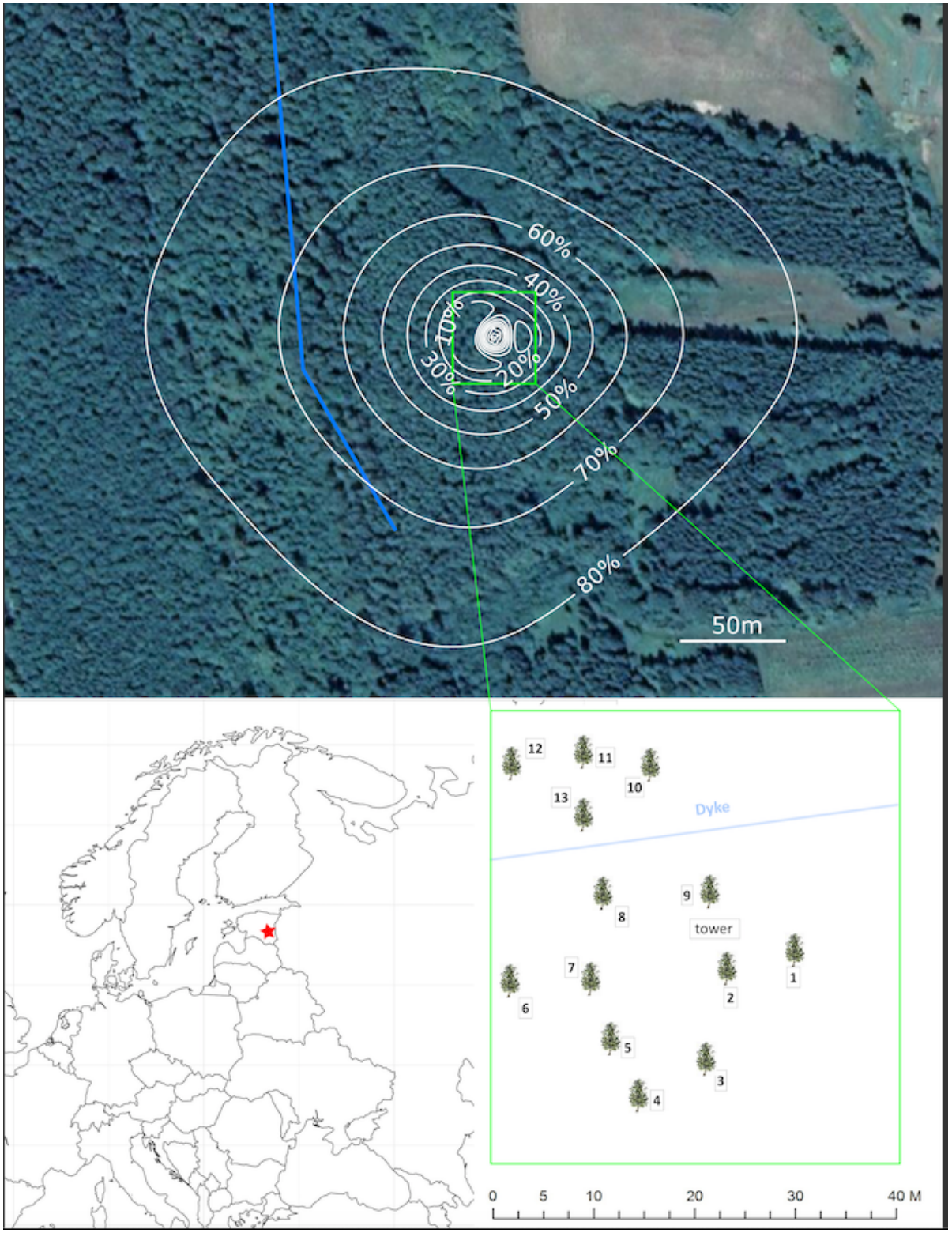

Figure 9

Location and research set-up of the riparian grey alder forest in Agali, Estonia. The automated soil chambers, the studied trees with chambers and the eddy tower with its footprint area are shown. The blue line indicates the stream (tributary of the Kalli River). For photos of set-up see Fig. S7.

Supplementary Files

This is a list of supplementary files associated with this preprint. Click to download.

- ManderetalforNCCSupplementaryMaterials.docx